1478–1487 *Nucleic Acids Research, 2007, Vol. 35, No. 5* *Published online 6 February 2007*
doi:10.1093/nar/gkm018

A rapid reaction analysis of uracil DNA glycosylase indicates an active mechanism of base flipping

Stuart R. W. Bellamy, Kuakarun Krusong and Geoff S. Baldwin*

Division of Molecular Biosciences, Sir Alexander Fleming Building, Imperial College London, South Kensington, London SW7 2AZ, UK

Received November 10, 2006; Revised December 20, 2006; Accepted January 2, 2007

ABSTRACT

Uracil DNA glycosylase (UNG) is the primary enzyme for the removal of uracil from the genome of many organisms. A key question is how the enzyme is able to scan large quantities of DNA in search of aberrant uracil residues. Central to this is the mechanism by which it flips the target nucleotide out of the DNA helix and into the enzyme-active site. Both active and passive mechanisms have been proposed. Here, we report a rapid kinetic analysis using two fluorescent chromophores to temporally resolve DNA binding and base-flipping with DNA substrates of different sequences. This study demonstrates the importance of the protein–DNA interface in the search process and indicates an active mechanism by which UNG glycosylase searches for uracil residues.

INTRODUCTION

Uracil DNA glycosylase (UNG) is responsible for the removal of uracil from DNA by hydrolysis of the N-glycosidic bond that links the base to the deoxyribose backbone, leaving an abasic site (1). Abasic sites are themselves potentially mutagenic and are repaired by the base excision repair pathway (2). UNG is a highly conserved enzyme found in many species. Detailed studies have been performed on the human (h), *E. coli* and herpes simplex virus type 1 (HSV-1) enzymes that are highly homologous at both the amino acid and structural levels (3–6).

All characterized UNG enzymes appear to have very similar properties: they are able to cleave uracil from both single- and double-stranded DNA, whether it is in a U·A base pair or any type of base mismatch (7–9). UNGs have an active site pocket that is highly specific for uracil (3,4). This prevents UNG from cleaving any normal bases from DNA, or indeed uracil from RNA. The enzyme binds uracil by flipping the target nucleotide out of the double helix and into the active site pocket via the major groove (5). The precise mechanism of nucleotide flipping has been the subject of intense debate (10–18).

Nucleotide flipping has been qualitatively described in the anthropomorphic terms of 'pushing' and 'pulling'. Energetically, an enzyme can destabilize the stacked conformation, equivalent to a 'push', or stabilize the unstacked conformation, equivalent to a 'pull'. Further, the act of destabilizing the stacked conformation implies an 'active' engagement of the enzyme in promoting base-flipping, whereas the stabilization of the unstacked conformation may give a completely 'passive' role for the enzyme, whereby it merely captures a base whilst it is in an extra-helical conformation. Estimates of the energetics of flipping a base are in the order of several times the thermal energy, kT, so that active participation of an enzyme in flipping a base is not an absolute requirement (19,20).

Structural analysis of hUNG bound to DNA revealed that in flipping the target nucleotide, the enzyme also compressed the DNA backbone through phosphate interactions either side of the target uracil. This 'pinch' could provide a direct mechanism for destabilizing the stacked base, actively promoting base-flipping (13). A highly conserved leucine loop also intercalates into the DNA helix, and may provide a 'push' (5). Rapid kinetic analyses have also concluded that UNG employs an active mechanism in flipping uracil from the DNA helix (15). However, a more recent study has suggested that UNG merely captures the base as it spontaneously flips whilst the enzyme is bound to the DNA, so that the enzyme is completely passive (11,14).

Studies with other base-flipping enzymes have suggested that there may be different mechanisms employed. Many other DNA repair enzymes are known to flip DNA bases (18), and there is strong evidence that some employ an active search mechanism (21–23). DNA methyltransferases, the first enzymes identified as base-flippers, methylate either cytosine or adenine bases at

*To whom correspondence should be addressed. Tel: +(44) 20 7594 5228; Fax: +(44) 20 7584 2056; Email: g.baldwin@imperial.ac.uk
Present addresses:
Stuart R.W. Bellamy, Department of Biochemistry, University of Bristol, Bristol BS8 1TD, UK.
Kuakarun Krusong, Department of Biochemistry, Faculty of Science, Chulalongkorn University, Bangkok 10330, Thailand.

defined sequences. Studies with EcoRI and M.EcoKI have demonstrated that bending of the DNA conformation is required for base flipping, in line with an active role for the enzyme (24,25). The HhaI methylase has been studied by ^{19}FNMR relaxation and data are consistent with passive flipping and trapping (26), although more recent studies suggest an active mechanism (27,28). A purely passive mechanism has been proposed for the α- and β-glucosyltransferase enzymes (16,17) as the intercalating loop on these enzymes enters the DNA on the same side from which the base must be everted. Active flipping through DNA distortion is excluded on the basis of minimal contacts in a non-specific mismatch complex, where the base is extra-helical, but not bound in the enzyme-active site, although much more extensive protein–DNA contacts exist in the specific enzyme–DNA complex (17). There are thus considerable differences in interpretation and there remains a lack of information regarding the dynamics of interactions at the protein–DNA interface, which are key to understanding the biophysical basis of base flipping.

To further examine the dynamics of the protein–DNA interface in base flipping by UNG, we have performed a rapid kinetic analysis with DNA substrates of different sequence. Previous biochemical studies have demonstrated that UNG is very dependent on the sequence context of the target uracil (29,30), in fact this is a greater determinant in catalytic efficiency than base pairing (9). We have previously examined this sequence discrimination using oligonucleotide substrates where the target uracil has been placed in either an AT- or GC-rich sequence context. Both the double- and single-stranded forms of these two substrates displayed similar properties towards UNG, with the GC-rich substrates having a consistently higher K_M (9).

Here, we have examined the sequence-dependent activity of UNG in greater detail, with the aim of further understanding the importance of the protein–DNA interface in base flipping. We have used single-stranded DNA, the preferred substrate for UNG, where the energetic barrier to base eversion will be reduced. Interactions with the DNA backbone will thus be of greater significance than intercalation of the leucine loop. We have used oligonucleotides with two fluorescence chromophores to provide temporal delineation of DNA binding and base eversion, and quench flow to follow hydrolysis of the N-glycosidic bond. Data have been analysed using a global fitting analysis that has enabled us to define the rates of the individual steps in the reaction pathway.

MATERIALS AND METHODS

Protein and DNA preparation

HSV-1 UNG wild-type and the D88N/H210N mutant were purified and stored as described earlier (9). Constructs containing the wild-type and mutant UNG genes were supplied by R. Savva. Oligonucleotides, including all modifications, used in the stopped-flow and quench-flow experiments (Table 1) were synthesized by MWG Biotech. Oligonucleotides were purified by HPLC as described earlier (31).

Table 1. Oligonucleotides used in this study

Abbreviation	Sequence
1U	5′-GAC TA***P*** **U**AA TGA CTG CG-3′
1HU	5′-(HEX) GAC TA***P*** **U**AA TGA CTG CG-3′
2U	5′-GAG GC***P*** **U**CC ACG CTG CG-3′
2HU	5′-(HEX) GAG GC***P*** **U**CC ACG CTG CG-3′
1N	5′-GAC T***P***A **U**AA TGA CTG CG-3′
3U	5′-^{32}P GAC TAA **U**AA TGA CTG CG-3′
4U	5′-^{32}P GAG GCG **U**CC ACG CTG CG-3′

Oligonucleotides were synthesized containing the chromophore 2-aminopurine (P) incorporated adjacent to the target uracil or with chromophore hexachlorofluorescein (HEX) incorporated at the 5′ end during synthesis.
U, 2′ deoxyuridine; P, 2-aminopurine (2-AP); HEX, hexachlorofluorescein.

Equilibrium fluorescence analysis

The fluorescent states of 2-aminopurine (2-AP) were measured on a SPEX Fluoromax spectrofluorometer using a 5-mm cuvette. The 2-AP fluorescence was recorded with an excitation wavelength of 310 nm and an emission wavelength of 368 nm. Excitation and emission slit widths were set at 0.9 and 1.5 mm, respectively. Titrations were performed at 25°C in reaction buffer (50 mM Tris pH 8.0, 1 mM EDTA, 150 mM NaCl).

Stopped-flow analysis

Stopped-flow experiments were performed on a TGK Scientific (formerly HI-TECH) SF-61DX2. Fixed concentrations of DNA were rapidly mixed with increasing concentrations of the D88N/H210N mutant HSV-1 UNG. All reactions were performed in reaction buffer (50 mM Tris pH 8.0, 1 mM EDTA, 150 mM NaCl) at 25°C. 2-AP fluorescence was obtained by exciting at 310 nm and collecting through a 340-nm interference filter; up to 10 transients were collected and averaged for each condition. Background signal was determined against buffer to allow scaling of the data. The observed rate (k_{obs}) was determined by fitting the averaged transients to the first-order rate equation using Grafit 5.0 (Erithacus software).

Stopped-flow anisotropy experiments were performed using a T-format with excitation and emission polarizers setup and signals calibrated according to the manufacturer's instructions. Fluorescence from hexachlorofluorescein (HEX) was obtained by exciting at 530 nm and collecting the emission through a WG540 cut-off filter (Comar); up to 15 transients were collected and averaged for each condition. The data from each channel was collected and mathematically converted by the KinetAssyst 3 software (TGK Scientific) to anisotropy and total fluorescence.

Global fitting

Berkeley Madonna was used to globally fit the stopped-flow fluorescence and anisotropy data. A model

that describes the binding and formation of a specific enzyme–DNA complex from Scheme 1 was written using a series of differential equations (Supplementary Data). A second model was also written to account for the complete reaction cycle as defined by Scheme 1 (Supplementary Data).

A complication arises when fitting changes in anisotropy if there is an associated change in fluorescence intensity, since each fluorescent state will then contribute unequally to the observed anisotropy. Hence the change in anisotropy will not follow the expected response unless it is corrected for the relative fluorescence contribution of each state. This has been accounted for in our global fit analysis.

^{32}P 5′-oligonucleotide labelling

Fifty picomoles of oligonucleotides 3U and 4U (Table 1) was 5′ phosphorylated with 25 pmol γ^{32}P [ATP] using T4 polynucleotide kinase (PNK). The reaction was performed in PNK buffer (25 mM $MgCl_2$, 25 mM DTT, 250 mM glycine-NaOH, pH 9.0) and incubated for 30 min at 37°C. The reaction was stopped with 50 mM EDTA and the labelled DNA was purified from any free γ^{32}P [ATP] using Bio Rad micro bio-spin 6 columns, which were spun at 3200 r.p.m. for 2 min.

Quench-flow analysis

UNG cleavage assays were performed using a HI-TECH RQF-63 rapid quench flow. All reactions were carried out in reaction buffer (50 mM Tris pH 8.0, 1 mM EDTA, 150 mM NaCl, 0.1 mg·ml^{-1} BSA) at 25°C. Reactions were quenched with 0.15 M NaOH at programmed time points, ranging from 0.05 to 100 s. The abasic sites formed after cleavage by UNG were cleaved by heating the alkaline solution to 90°C for 30 min. Cleaved DNA products were resolved from substrate by gel electrophoresis on a denaturing 18% polyacrylamide gel. The gels were exposed overnight on a Molecular Dynamics PhosphorImager and quantitated using ImageQuant.

Quench-flow data were fitted to a rectangular hyperbola, as defined by Equation (1), using Grafit5 (Erithacus Software).

$$k_{\text{obs}} = \frac{k_{cl}.[\text{E}]}{K_{\text{c}} + [\text{E}]} \quad (1)$$

where k_{obs} is the observed rate, E is the enzyme concentration, k_{cl} is the rate of N-glycosidic bond cleavage and K_{c} is equal to the enzyme concentration at ½ k_{cl}. (K_{c} is mathematically comparable to K_{M}, but it is not directly equivalent, since reactions are being performed with enzyme in excess and the complete reaction cycle is not being analysed).

RESULTS AND DISCUSSION

Defining the fluorescent states of 2-aminopurine

We have used substrates containing the fluorescent base analogue 2-AP as a means to follow the interactions of UNG with its substrate, a 2′-deoxyuracil residue within DNA. It has been shown in previous studies from both this lab and others that the fluorescence of 2-AP, when adjacent to uracil, provides a signal that can be used to follow the cleavage of the uracil from the DNA by UNG (9,32).

We wished to define more precisely the changes in 2-AP fluorescence intensity in relation to the different states of the DNA as substrate, product and enzyme complexes. We therefore defined the emission coefficients for the possible physical states of the fluorescent DNA. This was performed by titrating increasing concentrations of DNA, or enzyme–DNA complexes, into a cuvette and measuring the fluorescence intensity. Plotting the fluorescence intensity against concentration produces a straight line, the gradient of which defines the emission coefficient under the conditions used (Figure 1). [Note that emission coefficients are not standardized, since they are dependent upon numerous factors that affect the sensitivity of the instrument used, as well as the settings used during data collection. However, the relative emission coefficients (shown in Table 2) are ratios of emission coefficients and will be reproducible on other fluorospectrophotometers, provided that data are collected in an appropriate manner.]

We have determined the emission coefficients for both the uracil-containing substrate oligonucleotides (1U and 2U; Table 2), as well as their abasic products (1-AP and 2-AP) and a control, where the 2-AP is not immediately adjacent to the target uracil (1N). In addition, the emission coefficients for different enzyme–DNA complexes have been determined by titrating in fixed ratios of enzyme and DNA. Since it is not possible to analyse specific enzyme–substrate complexes with wild-type UNG, an inactive mutant of UNG was used, where both the catalytic residues had been mutated to Asn (D88N/H210N). We have demonstrated earlier that this mutant does not support catalysis, but that it binds tightly to substrate DNA (8,9), and hence is ideal for investigating enzyme–substrate interactions. Enzyme–product complexes were analysed with both wtUNG and D88N/H210N UNG. The concentration of enzyme was always kept in excess of the concentration of DNA and experiments were performed under conditions such that the DNA would be bound; appropriate concentrations were calculated from our previously determined values of K_{d} for these substrates (9).

Inspection of the data from these titrations reveals that the free substrates 1U and 2U have different slopes from their respective products 1-AP and 2-AP, whilst the steepest slopes are observed with the specific enzyme–DNA complexes formed by D88N/H210N UNG (Figure 1A and C). These experiments reveal that steep slopes are also obtained with the product oligonucleotides and that wtUNG and D88N/H210N UNG give very similar results (Figure 1B and D). Examination of the 1N control oligonucleotide showed that the free and D88N/H210N UNG complexed oligonucleotide had the same emission coefficient, demonstrating that the fluorescence changes that we are observing are specific for the conformational changes associated with the target uracil,

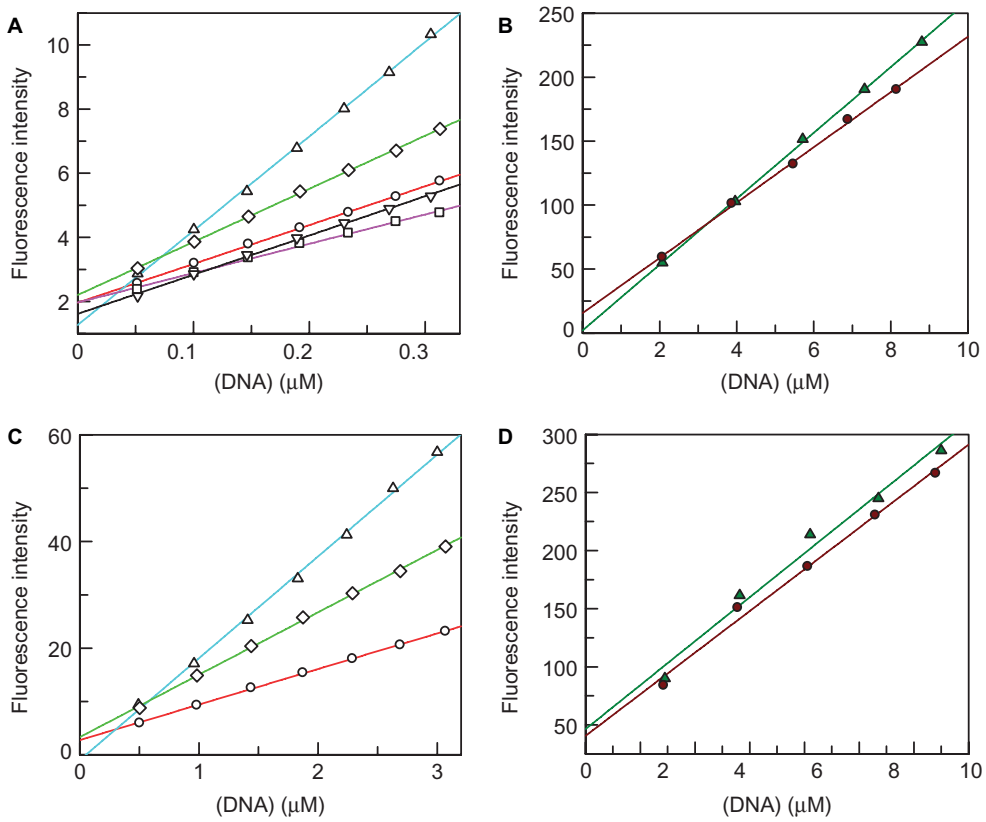

Figure 1. Fluorescence states were determined by titrating increasing concentrations of oligonucleotides 1U (panels **A** and **B**) and 2U (panels **C** and **D**), or fixed ratios of oligonucleotides and enzyme, and observing the change in fluorescence. All data are shown with the best fit to a linear equation. Fluorescence states were assigned for free substrate (open circles, red line), the specific E·S complex (open triangles, cyan line), the free abasic product (open diamonds, green line), the E·P complex with both wild-type UNG (closed circles, maroon line) and the D88N/H210N mutant (closed triangles, dark green line). The control oligonucleotide (1N) with 2-AP not adjacent to the target uracil was also examined as free DNA (open squares, magenta line), and in an enzyme–DNA complex (open inverted triangles, black line).

Table 2. Quantitative analysis of the fluorescent states of 2-aminopurine

State	Increase in fluorescence (nM)		Ratio (compared to free [S])	
	1U	2U	1U	2U
Free S	105.3	66.7	1.0	1.0
D88N/H210N·S complex	248.5	191.0	2.36	2.86
WT·P complex	216.0	178.9	2.05	2.68
D88N/H210N·P complex	257.3	188.9	2.44	2.83
Free P	144.1	117.1	1.37	1.66
Free 1N	91.4	–	0.87	–
D88N/H210N·1N complex	122.3	–	1.16	–

Mixing fixed ratios of oligonucleotides 1U or 2U and UNG in increasing concentrations resulted in a linear increase in 2-AP fluorescence. The gradient of this increase can be used to calculate the ratio of the level of fluorescence of any state to that of free substrate. Hence the fluorescent states of 1U or 2U can be quantitatively compared.

and are not due to non-specific enzyme–DNA interactions (Figure 1A).

A summary of these experiments is shown in Table 2, with the calculated relative emission coefficient. The lowest fluorescent state is defined by the free uracil-containing substrate oligonucleotide. An intermediate fluorescent state is observed for the free abasic product DNA, which has a 1.37–1.66-fold enhancement over the substrate DNA. It is this difference that accounts for the signal used in the steady-state experiments (9). The highest fluorescent state arises from the formation of the specific enzyme–DNA complex and is the same for both enzyme–substrate and enzyme–product complexes, with an average fluorescence enhancement of 2.45-fold over the free substrate oligonucleotides. Although we observe a slightly lower relative emission coefficient with wtUNG and product 1U, we do not believe that this is significant, since we do not observe a similar reduction with wtUNG

and the product of 2U. This analysis clearly reveals that there are three fluorescent states for the oligonucleotides that we have used in this study: free substrate (low), free product (intermediate) and an enzyme-bound specific DNA complex (high).

We observe similar values in absolute fluorescence intensity with both substrates and similar changes on going from the single-stranded substrate to an enzyme–DNA complex and the abasic product (Figure 1). This indicates that there is significant quenching of 2-AP in the single-stranded substrates 1U and 2U, and that similar structural transitions occur with both substrates on reaction with UNG that reduce this quenching effect. 2-AP fluorescence intensity is sensitive to the structure of DNA and quenching is observed within an oligonucleotide due to both stacking and collisional interactions with neighbouring bases (33). Changes in fluorescence intensity occur when the structure of DNA is altered, which can include base flipping as well as other structural perturbations (34). Since the change in 2-AP fluorescence can here be correlated with structural data (3,5), and a negative control (Figure 1A), a reliable assignment of the high-fluorescence intermediate can be made to the eversion and binding of the neighbouring uracil by UNG. Although it may seem somewhat illogical to discuss base-flipping with single-stranded DNA substrates, the changes in fluorescence intensity that we observe demonstrate that there must be significant secondary structure in the DNA substrates. A similar structural transition will therefore be required to bind the target uracil within the enzyme-active site. However, the energetic barrier to this 'flipping' would be expected to be considerably less with single-stranded DNA rather than double-stranded DNA.

The intermediate level fluorescence observed in the abasic product is also consistent with reduced nucleotide interactions and increased solvent exposure expected due to the presence of an abasic site next to the 2-AP. These data also imply that there will not be a significant 2-AP fluorescence signal corresponding to the chemical cleavage step in the enzyme pathway and we demonstrate below that this is indeed the case.

Global analysis of substrate DNA binding

The initial encounter of enzyme and DNA will be a second-order binding event to form a non-specific complex. Formation of the specific enzyme–DNA complex characterized by the high 2-AP fluorescence state must then occur as a subsequent first-order process, as in Scheme 1 below.

$$\mathrm{E} + \mathrm{S} \underset{k_{-1}}{\overset{k_1}{\underset{\Delta r\ \Delta I_{\mathrm{H}}}{\rightleftharpoons}}} \mathrm{E}\cdot\mathrm{S} \underset{k_{-2}}{\overset{k_2}{\underset{\Delta I_{2\mathrm{AP}}}{\rightleftharpoons}}} \mathrm{E}\cdot\mathrm{S}^{*} \xrightarrow{k_{\mathrm{cl}}} \mathrm{E}\cdot\mathrm{P} \xrightarrow{k_{\mathrm{off}}} \mathrm{E} + \mathrm{P} + \mathrm{U}$$

(Scheme 1)

where the enzyme (E) binds the substrate DNA (S) to form a non-specific enzyme–substrate complex (E·S), that may then proceed to the specific complex (E·S*). Cleavage of the N-glycosidic bond results in an enzyme–product complex (E·P) which, following dissociation, leads to the free enzyme, the abasic DNA product (P) and uracil (U).

The 2-AP fluorescence states described in Figure 1 report on the formation of the specific enzyme–DNA complex E·S*, but provides no information on the non-specific intermediate E·S. To deconvolute the conformational change associated with base flipping from non-specific complex formation thus requires a different signal that is sensitive only to DNA binding.

Fluorescence anisotropy monitors the extent to which plane polarzied light is depolarized due to the tumbling of a molecule in solution between excitation and emission (35). DNA labelled on the 5′ end with HEX has proved to be a very useful probe for investigating DNA binding (36), and we have previously used it in equilibrium binding studies of UNG (8,9). The use of the two chromophores, 2-AP and HEX, can thus be used to provide temporal resolution between DNA binding and base flipping (37). The initial binding of the enzyme and DNA leads to a change in the anisotropy (Δr) and total HEX fluorescence (ΔI_{H}), subsequent conformational changes that lead to base flipping and formation of the specific enzyme–DNA complex then produce a change in 2-AP fluorescence ($\Delta I_{2\mathrm{AP}}$). These different fluorescence signals thus report on different steps in the reaction pathway.

Previous rapid kinetic studies have demonstrated that the transition from non-specific to a specific complex, denoted by k_2 in Scheme 1, is very rapid (14,15). Delineation between the first- and second-order rates is in theory possible at high concentrations where the second-order binding, monitored by HEX anisotropy, will be faster than the first-order base-flipping, monitored by 2-AP fluorescence. The former will increase linearly with concentration, while the latter will ultimately give a hyperbolic response as the E·S complex saturates. Fitting of such hyperbolic data may be performed with an equation derived from Scheme 1, using the square root approximation, and requires that the experiments are performed under pseudo first-order conditions, as described by Johnson (38). The limiting factor on such an analysis is the dead-time of stopped-flow machines which are in the 1-ms range. At even moderate concentrations, and hence rates, most of the signal becomes lost in the dead-time of the instrument, as demonstrated below.

While this approach has been applied earlier to *E. coli* UNG (15), it did not appear likely that it would be sensitive enough to deconvolute the differences in DNA-binding and -flipping events between the 1U and 2U substrates that we were examining here. Furthermore, the significant differences observed between the two substrates indicated that substrate 2U was not reaching saturation in DNA binding under accessible conditions (data not shown and below), so that pseudo first-order conditions would not be possible to fulfill.

To overcome these limitations, we have employed a strategy based on a global fit of both 2-AP fluorescence and anisotropy data using numerical integration of a kinetic model. Numerical integration has the advantage that it does not require any assumptions to solve a mathematical equation. Furthermore, it does not require that experiments are performed under pseudo first-order

conditions, since the conditions are inherently accounted for in the model. Under non-saturating conditions, a reversible system will reach an equilibrium position that is not at the end-point, with the important consideration being that amplitudes are critical in the subsequent data analysis.

We performed stopped-flow experiments using the catalytically deficient D88N/H210N HSV-1 UNG. Fixed concentrations of oligonucleotides 1HU and 2HU (Table 1) were mixed with increasing concentrations of enzyme. A dual detection setup enabled the simultaneous acquisition of the horizontal and vertical components of the HEX fluorescence, allowing the acquisition of time-resolved anisotropy data. The same enzyme and DNA solutions were then used to acquire 2-AP fluorescence data in a conventional fluorescence setup. The data were treated to produce anisotropy (r), total HEX fluorescence (I_H) and 2-AP fluorescence (I_{2AP}), each as a function of enzyme concentration and for each substrate (Figure 2).

These data were fitted by numerical integration to a kinetic model using Berkeley Madonna. This enabled the simultaneous fitting of anisotropy, total HEX fluorescence and 2-AP fluorescence at different enzyme concentrations: rate constants were thus determined by the simultaneous fitting of 18 000 data points. The model used to fit these data was based on Scheme 1, but omitting the cleavage and subsequent steps, since an inactive mutant was used (Supplementary Data).

The model produced a very good fit for the anisotropy and total HEX fluorescence, which defines the initial encounter between enzyme and substrate (Figure 2). The fit to the 2-AP fluorescence was good, but exhibited some systematic deviation (Figure 2). This is consistent with other 2-AP data that was collected under pseudo first-order conditions, which required a fit to a single exponential plus slope to produce the best fit (data not shown). This is most likely due to a slower conformational change that follows the initial transition to the high-fluorescence intermediate. This slower change is not necessarily accompanied by a change in the fluorescence state of E·S*, as the intensity change may be a kinetic effect due to the further accumulation of the high-fluorescence intermediate. Alternative models were tested that would account for a further equilibrium step, but these did not produce a better fit to the data. Furthermore, the lack of an independent signal to define a further intermediate led to an undesirable ambiguity in the fitted rates. It was therefore concluded that the model which relates to Scheme 1 was the simplest that could accurately account for the observed data with no ambiguity in the fitted rate constants.

A clear distinction between the 1HU and 2HU substrates emerges when the rates determined from the global analysis are examined (Table 3). The initial encounter between enzyme and DNA is the same for each substrate since the second-order binding rate k_1 is in both cases approaching the diffusion-controlled rate limit. The reverse rate k_{-1} is larger with the GC-rich 2HU substrate indicating that non-specific E·S complex may be rather less stable, although this should not be over-interpreted since fitting is relatively insensitive to this rate. Thereafter the progression from the non-specific E·S complex changes dramatically between the substrates: the forward rate k_2 to produce the high-fluorescence E·S* complex is very fast with 1HU, but more than 10-fold slower with 2HU. This demonstrates that once the non-specific E·S complex has been formed, UNG is able to form the activated E·S* complex at a much lower energetic cost with 1HU than 2HU. The poor activity demonstrated by UNG towards the 2U substrate can thus be attributed to an increased energetic cost in base flipping and formation of the activated complex. This is consistent with the increased K_M for this substrate (9).

Quench-flow analysis

The stopped-flow analysis above provides an insight into the binding of substrate and the formation of the activated complex. Further examination of the reaction cycle requires analysis of the chemical cleavage step. The use of quench flow allows just such an investigation. Enzyme and DNA are mixed, and following a fixed time are then chemically quenched with NaOH. This immediately inactivates the enzyme, and on heating to 90°C results in cleavage of abasic product DNA, whilst leaving substrate intact. Substrate and product can then be separated by denaturing PAGE and quantified by storage phosphor autoradiography. By performing quench-flow experiments on both AT- and GC-rich single-stranded DNA substrates, the effect of sequence context on the rate of chemical hydrolysis of deoxyuridine was examined.

Quench-flow reactions were performed using fixed concentrations of ^{32}P radiolabelled single-stranded oligonucleotides 3U and 4U (Table 1) and increasing amounts of wild-type UNG. Experiments were performed with fixed concentrations of substrate and increasing concentrations of enzyme. The rates determined for each reaction were then plotted as a function of substrate concentration. With the AT-rich substrate 3U, the observed rates showed a hyperbolic increase with enzyme concentration (Figure 3A), the data was thus fitted to a rectangular hyperbola, defined by Equation (1). The value of k_{cl} determined from this represents the rate of the actual chemical cleavage step for UNG.

With the GC-rich substrate 4U, no hyperbolic response was observed, demonstrating that the enzyme was not reaching saturation with this substrate, even at very high enzyme concentrations (Figure 3B). This is consistent with the response observed for the GC-rich substrate in the global fluorescence analysis (Figure 2), which failed to reach saturation.

The complete reaction cycle of UNG

The kinetic analyses described above have provided an examination of the reaction steps leading to the formation of an enzyme–product complex. The final step that completes the reaction cycle is the dissociation of enzyme and product. We have investigated the complete reaction cycle of UNG by using wild-type UNG and monitoring the 2-AP stopped-flow fluorescence under

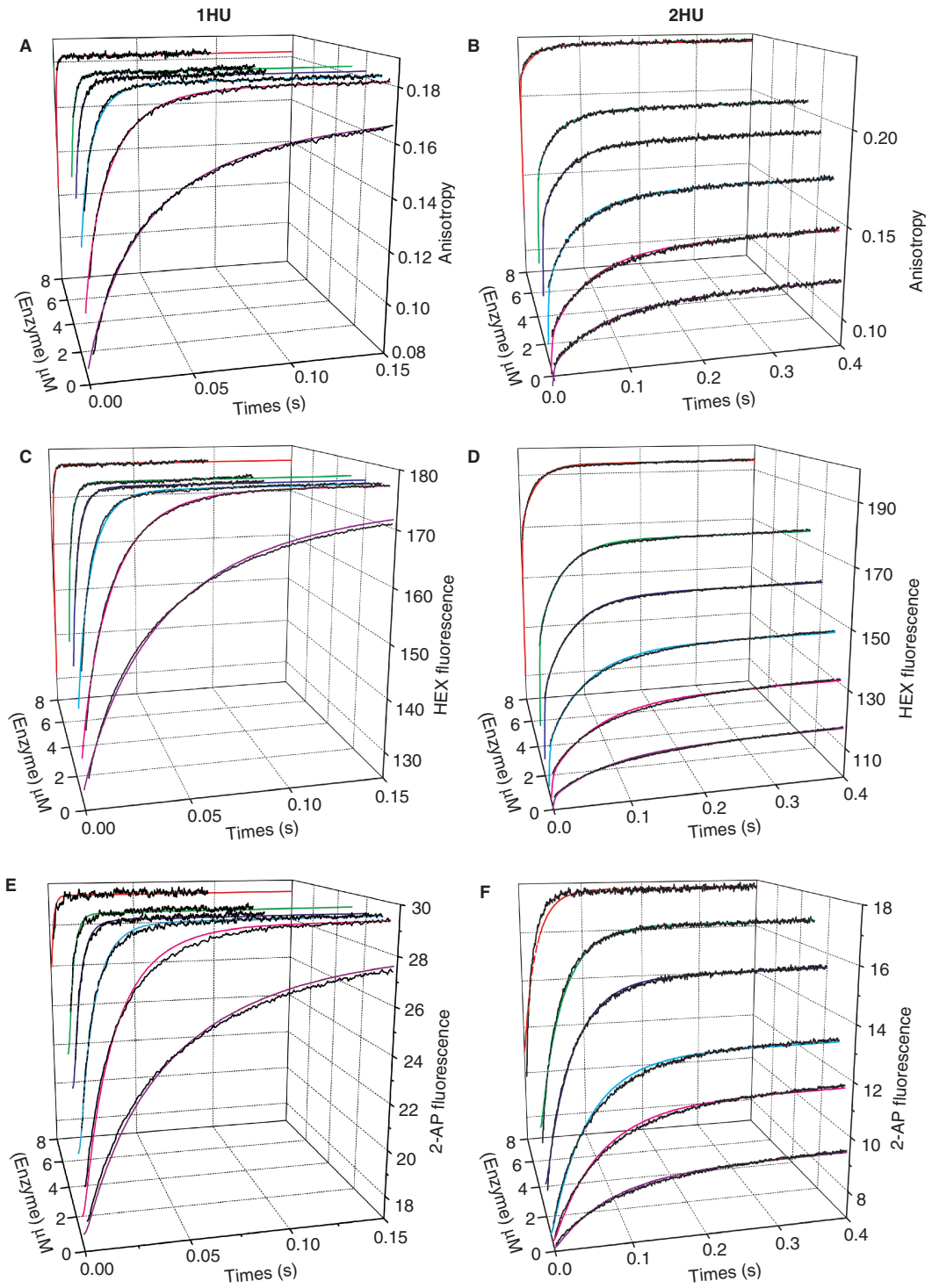

Figure 2. Substrates 1HU (left column) and 2HU (right column) were mixed with increasing concentrations of D88N/H210N UNG using stopped-flow. Anisotropy (**A** and **B**) and total HEX fluorescence (**C** and **D**) were simultaneously monitored, and the same solutions were then used to collect 2-AP fluorescence (**E** and **F**). The data are shown with the results of a global fit to Scheme 1. Individual curves for each of the enzyme concentrations used are shown: 8 μM (red); 3 μM (green); 2 μM (blue); 1 μM (cyan); 0.5 μM (magenta) and 0.2 μM (purple), all reactions were performed with 0.1 μM substrate and other conditions as described in the Materials and methods section.

a full reaction cycle with equimolar amounts of enzyme and substrates 1U or 2U. The different fluorescence states of 2-AP generated during the UNG reaction were observed, and these can be assigned to specific steps in the UNG reaction, as defined by the relative intensities of the 2-AP-containing DNA in different states and complexes (Table 2). An initial increase is observed that corresponds to the rapid increase in fluorescence resulting

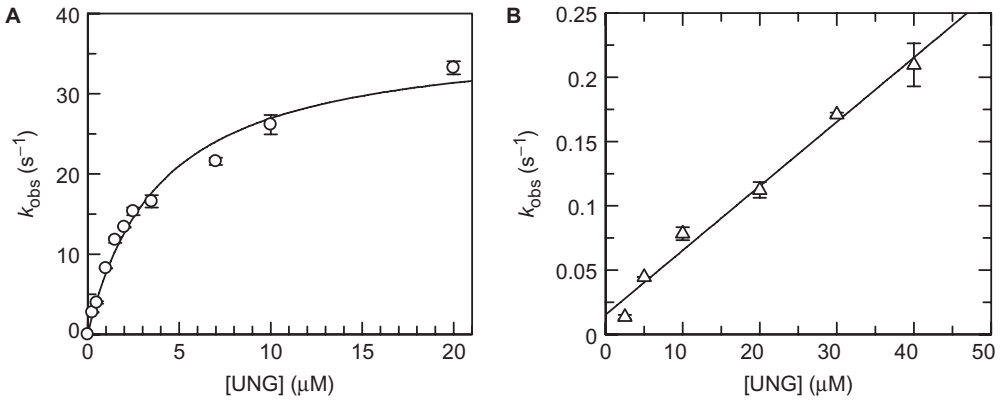

Figure 3. Rates of chemical cleavage were determined by mixing UNG and either substrate 3U (**A**) or 4U (**B**). The observed rates (k_{obs}) are plotted against enzyme concentration. (**A**) Data for the AT-rich single-stranded oligonucleotide 3U is shown with the best fit to Equation (1), with values of $k_{cl} = 37.5 \pm 1.8\,s^{-1}$ and $K_c = 3.9 \pm 0.5\,\mu M$. (**B**) The data for the GC-rich single-stranded oligonucleotide 4U did not reach saturation and exhibited a linear rather than hyperbolic relationship, hence is shown with the best fit to a linear equation.

Table 3. Rate constants determined from global fitting

	Substrate	
Rate constant	1HU	2HU
$k_1\,M^{-1}\,s^{-1}$	1.54×10^8	0.835×10^8
$k_{-1}\,s^{-1}$	62.0	390
$k_2\,s^{-1}$	670	48.1
$k_{-2}\,s^{-1}$	16.3	13.5

from the formation of the specific UNG–DNA complex from the free DNA. A subsequent decrease in fluorescence is then observed, corresponding to the decrease in fluorescence that results from dissociation of the abasic DNA product after catalysis has occurred (Figure 4). The final fluorescence is higher than the starting fluorescence, corresponding to the increase in fluorescence between substrate and product DNAs (cf. Figures 1 and 4).

Reaction Scheme 1 describes the complete reaction cycle of UNG. We have extended the Berkeley Madonna model used to describe this reaction scheme to also include the hydrolysis and product dissociation steps (Supplementary Data). This was then used to fit the 2-AP fluorescence data obtained with wild-type enzyme. The values for k_1, k_{-1}, k_2 and k_{-2} were taken from the global analysis (Table 3). The value for k_{cl} was taken from the quench-flow analysis with 3U (Figure 3), and was assumed to be the same for each substrate since this defines the rate of a chemical process. The starting fluorescence for each substrate was normalized to a value of ~1, and fitting was used to determine the off-rate (k_{off}) and the relative fluorescence intensities of the free substrate (I_{2APD}), enzyme-bound substrate (I_{2APDE}) and free product (I_{2APP}). Fitting only this small number of parameters produced excellent fits to the reaction data (Figure 4). Normalizing the starting values of the fluorescence enabled a comparison of the relative fluorescence intensities of the intermediates determined from this fitting (Table 4). These correspond extremely well with the values of relative fluorescence intensity for the different DNAs and enzyme–DNA complexes determined under equilibrium conditions (Table 2). This analysis with wild-type enzyme and substrate importantly demonstrates the validity of the overall kinetic model in describing the reaction pathway.

Implications for damage recognition and base flipping by UNG

The process by which DNA glycosylases are able to locate damaged bases within large amounts of undamaged DNA remains one of the enigmas of DNA repair. This study has investigated the reaction pathway of UNG with uracil residues located in different sequence contexts, and provides a new insight into the steps prior to excision of the base.

The critical step in the reaction pathway is the formation of the specific enzyme–DNA complex, where the uracil base has been flipped into the enzyme-active site and catalysis may proceed. This is governed by the rate k_2 in Scheme 1, and is highly dependent on the sequence context of the target uracil (Table 3). The reduced rate for k_2 with the GC-rich substrate indicates an increased activation energy for this process.

The results reported here demonstrate that damage recognition by UNG is dependent upon the sequence context of the target uracil. The initial encounter of enzyme and DNA to form a non-specific complex is not greatly affected by the DNA sequence (k_1 and k_{-1}; Table 3). This binding will largely involve electrostatic forces and will not be dependent on intricate molecular recognition. Damage recognition is the process by which UNG forms the specific enzyme–DNA complex: this requires the flipping of the uracil from the DNA into the enzyme-active site. Much debate has centred around the mechanism of base flipping and the question of whether the enzyme plays an active or passive role in this process (5,11,13–18,25).

Structural analysis of UNG suggested a 'pinch–push–pull' mechanism for base flipping (5,13), later modified by

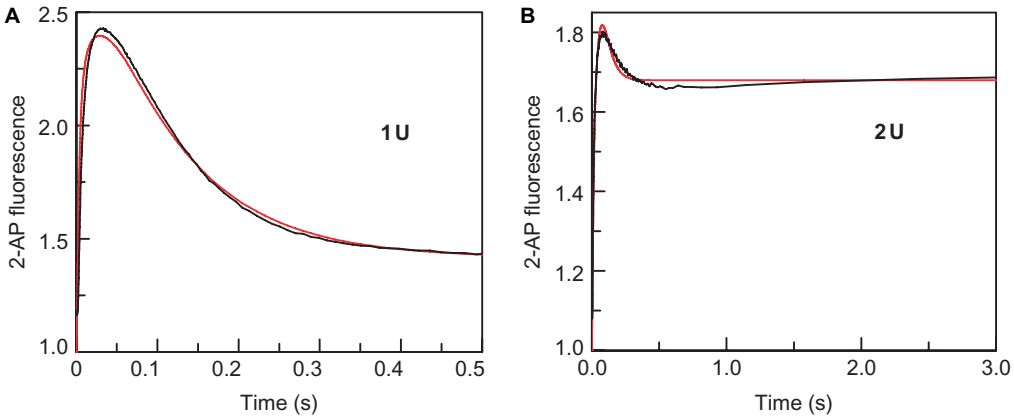

Figure 4. A complete reaction cycle of UNG was analysed by monitoring 2-AP fluorescence using stopped-flow to rapidly mixing equimolar amounts of wtUNG and substrates 1U (**A**) and 2U (**B**) at concentrations in excess of the K_M (4 μM 1U and 20 μM 2U). The data are shown with the best fit to Scheme 1 using kinetic parameters determined from the global stopped-flow analysis (Table 3), the cleavage rate determined from the quench-flow analysis (Figure 3), and fitting only a single kinetic parameter, the off-rate (k_{off}), together with the fluorescence coefficients for substrate (I_{2APD}), enzyme–substrate complex (I_{2APDE}) and product (I_{2APP}; Table 4).

Table 4. Fitting values from complete reaction cycle of UNG

	1U	2U
I_{2APD}	1.0	1.0
I_{2APDE}	2.60	2.46
I_{2APP}	1.42	1.68
k_{off}	9.48	43.5

kinetic analysis to a 'pinch–pull–push' mechanism. A more recent study concluded that UNG simply captures the base as it spontaneously flips whilst the enzyme is bound to the DNA (11,14). This is unexpected since one would expect the act of binding to DNA would affect the immediate environment and energetics of the DNA. Furthermore, the authors' data indicated a significant increase in the rate of base opening for a thymine when bound by UNG. However, the principle effect of the enzyme was to reduce the rate of base closure. This corresponds with kinetic studies that indicated the leucine loop intercalated after base-flipping, thus stabilizing the extra-helical conformation, rather than actively destabilizing ('pushing') the intra-helical conformation. There is thus some consensus in the role of UNG in stabilizing the flipped base through specific interactions with the uracil and the intercalating leucine loop, but whether UNG actively destabilizes ('pushes') the target base remains controversial.

The data we present here provide a new perspective in this debate. The rates k_2 and k_{-2} in Scheme 1 directly correlate to base opening and closure, respectively. Both of these substrates are single stranded, so the energetic barrier to base eversion will be lower than with a double-stranded substrate. Yet we see a significant difference between the rates of base opening between the two substrates, but not for base closure. This can only be due to differences in the rate of spontaneous base eversion, as in a passive mechanism, or modulation of the protein–nucleic acid interface due to differences in local DNA structure in an active mechanism. The former is unlikely given that the substrates are single stranded, and base stacking is stronger in single-stranded polyA DNA (14,39), which is more like the AT-rich 1U substrate. We have also concluded earlier that differences between the double-stranded forms of these two substrates are unlikely to be due to differences in helical stability (9). We therefore conclude that the large differences in the rates of base opening are due to differences in the protein–nucleic acid interface. This is supported by previous studies that have observed large K_M effects when the target uracil is placed within the unusual DNA structure of a hairpin (40,41). The logical conclusion therefore is that protein–DNA interactions are critical in uracil eversion that requires active engagement of the UNG enzyme with the DNA.

CONCLUSION

Conformational transitions associated with base flipping are naturally dynamic processes. To fully understand such processes therefore requires dynamic methods that can provide an insight into these transitions as they occur. This provides an alternative perspective and, in conjunction with structural techniques, is critical in obtaining a complete understanding of this important process in DNA damage recognition. We have demonstrated that these dynamic transitions are dependent upon DNA sequence. The protein–DNA interface is thus critical in modulating the energetics of base flipping, which is dependent upon an active role of the enzyme in affecting this structural transition.

SUPPLEMENTARY DATA

Supplementary Data is availabe at NAR Online

ACKNOWLEDGEMENTS

The authors would like to thank Steve Halford and Mark Szczelkun for their ever-insightful discussions and advice. We would also like to thank the BBSRC for

funding (98/A1/G/04058; JF09028; B11484) and equipment (REI BB/C510859/1).

Conflict of interest statement. None declared.

REFERENCES

1. Lindahl,T. (1974) An N-glycosidase from Escherichia coli that releases free uracil from DNA containing deaminated cytosine residues. *Proc. Natl. Acad. Sci. U.S.A.*, **71**, 3649–3653.
2. Seeberg,E., Eide,L. and Bjoras,M. (1995) The base excision repair pathway. *Trends. Biochem. Sci.*, **20**, 391–397.
3. Savva,R., McAuleyhecht,K., Brown,T. and Pearl,L. (1995) The structural basis of specific base-excision repair by uracil-DNA glycosylase. *Nature*, **373**, 487–493.
4. Mol,C.D., Arvai,A.S., Slupphaug,G., Kavli,B., Alseth,I., Krokan,H.E. and Tainer,J.A. (1995) Crystal structure and mutational analysis of human uracil-DNA glycosylase: structural basis for specificity and catalysis. *Cell*, **80**, 869–878.
5. Slupphaug,G., Mol,C.D., Kavli,B., Arvai,A.S., Krokan,H.E. and Tainer,J.A. (1996) A nucleotide-flipping mechanism from the structure of human uracil-DNA glycosylase bound to DNA. *Nature*, **384**, 87–92.
6. Xiao,G.Y., Tordova,M., Jagadeesh,J., Drohat,A.C., Stivers,J.T. and Gilliland,G.L. (1999) Crystal structure of Escherichia coli uracil DNA glycosylase and its complexes with uracil and glycerol: structure and glycosylase mechanism revisited. *Proteins*, **35**, 13–24.
7. Verri,A., Mazzarello,P., Spadari,S. and Focher,F. (1992) Uracil-DNA glycosylases preferentially excise mispaired uracil. *Biochem. J.*, **287**, 1007–1010.
8. Krusong,K., Carpenter,E.P., Bellamy,S.R., Savva,R. and Baldwin,G.S. (2006) A comparative study of uracil-DNA glycosylases from human and herpes simplex virus type 1. *J. Biol. Chem.*, **281**, 4983–4992.
9. Bellamy,S.R. and Baldwin,G.S. (2001) A kinetic analysis of substrate recognition by uracil-DNA glycosylase from herpes simplex virus type 1. *Nucleic Acids Res.*, **29**, 3857–3863.
10. Parikh,S.S., Putnam,C.D. and Tainer,J.A. (2000) Lessons learned from structural results on uracil-DNA glycosylase. *Mutat. Res.*, **460**, 183–199.
11. Cao,C., Jiang,Y.L., Stivers,J.T. and Song,F. (2004) Dynamic opening of DNA during the enzymatic search for a damaged base. *Nat. Struct. Mol. Biol.*, **11**, 1230–1236.
12. Stivers,J.T. and Jiang,Y.L. (2003) A mechanistic perspective on the chemistry of DNA repair glycosylases. *Chem. Rev.*, **103**, 2729–2759.
13. Parikh,S.S., Mol,C.D., Slupphaug,G., Bharati,S., Krokan,H.E. and Tainer,J.A. (1998) Base excision repair initiation revealed by crystal structures and binding kinetics of human uracil-DNA glycosylase with DNA. *EMBO J.*, **17**, 5214–5226.
14. Wong,I., Lundquist,A.J., Bernards,A.S. and Mosbaugh,D.W. (2002) Presteady-state analysis of a single catalytic turnover by Escherichia coli uracil-DNA glycosylase reveals a ''pinch-pull-push'' mechanism. *J. Biol. Chem.*, **277**, 19424–19432.
15. Stivers,J.T., Pankiewicz,K.W. and Watanabe,K.A. (1999) Kinetic mechanism of damage site recognition and uracil flipping by Escherichia coli uracil DNA glycosylase. *Biochemistry*, **38**, 952–963.
16. Lariviere,L., Sommer,N. and Morera,S. (2005) Structural evidence of a passive base-flipping mechanism for AGT, an unusual GT-B glycosyltransferase. *J. Mol. Biol.*, **352**, 139–150.
17. Lariviere,L. and Morera,S. (2004) Structural evidence of a passive base-flipping mechanism for beta-glucosyltransferase. *J. Biol. Chem.*, **279**, 34715–34720.
18. Roberts,R.J. and Cheng,X. (1998) Base flipping. *Annu. Rev. Biochem.*, **67**, 181–198.
19. Banavali,N.K., Huang,N. and MacKerell,A.D.Jr (2006) Conserved patterns in backbone torsional changes allow for single base flipping from duplex DNA with minimal distortion of the double helix. *J. Phys. Chem. B. Condens. Matter Surf. Interfaces Biophys.*, **110**, 10997–11004.
20. Banavali,N.K. and MacKerell,A.D.Jr (2002) Free energy and structural pathways of base flipping in a DNA GCGC containing sequence. *J. Mol. Biol.*, **319**, 141–160.
21. Banerjee,A., Santos,W.L. and Verdine,G.L. (2006) Structure of a DNA glycosylase searching for lesions. *Science*, **311**, 1153–1157.
22. Banerjee,A., Yang,W., Karplus,M. and Verdine,G.L. (2005) Structure of a repair enzyme interrogating undamaged DNA elucidates recognition of damaged DNA. *Nature*, **434**, 612–618.
23. Fromme,J.C., Banerjee,A. and Verdine,G.L. (2004) DNA glycosylase recognition and catalysis. *Curr. Opin. Struct. Biol.*, **14**, 43–49.
24. Allan,B.W., Garcia,R., Maegley,K., Mort,J., Wong,D., Lindstrom,W., Beechem,J.M. and Reich,N.O. (1999) DNA bending by EcoRI DNA methyltransferase accelerates base flipping but compromises specificity. *J. Biol. Chem.*, **274**, 19269–19275.
25. Su,T.J., Tock,M.R., Egelhaaf,S.U., Poon,W.C. and Dryden,D.T. (2005) DNA bending by M.EcoKI methyltransferase is coupled to nucleotide flipping. *Nucleic Acids Res.*, **33**, 3235–3244.
26. Klimasauskas,S., Szyperski,T., Serva,S. and Wuthrich,K. (1998) Dynamic modes of the flipped-out cytosine during HhaI methyltransferase-DNA interactions in solution. *EMBO J.*, **17**, 317–324.
27. Daujotyte,D., Serva,S., Vilkaitis,G., Merkiene,E., Venclovas,C. and Klimasauskas,S. (2004) HhaI DNA methyltransferase uses the protruding Gln237 for active flipping of its target cytosine. *Structure*, **12**, 1047–1055.
28. Huang,N., Banavali,N.K. and MacKerell,A.D.Jr (2003) Protein-facilitated base flipping in DNA by cytosine-5-methyltransferase. *Proc. Natl. Acad. Sci. U.S.A.*, **100**, 68–73.
29. Eftedal,I., Guddal,P.H., Slupphaug,G., Volden,G. and Krokan,H.E. (1993) Consensus sequences for good and poor removal of uracil from double-stranded DNA by uracil-DNA glycosylase. *Nucleic Acids Res.*, **21**, 2095–2101.
30. Nilsen,H., Yazdankhah,S.P., Eftedal,I. and Krokan,H.E. (1995) Sequence specificity for removal of uracil from U·A pairs and U·G mismatches by uracil-DNA glycosylase from Escherichia coli, and correlation with mutational hotspots. *FEBS Lett.*, **362**, 205–209.
31. Baldwin,G.S., Vipond,I.B. and Halford,S.E. (1995) Rapid reaction analysis of the catalytic cycle of the EcoRV restriction endonuclease. *Biochemistry*, **34**, 705–714.
32. Stivers,J.T. (1998) 2-Aminopurine fluorescence studies of base stacking interactions at abasic sites in DNA: metal-ion and base sequence effects. *Nucleic Acids Res.*, **26**, 3837–3844.
33. Rachofsky,E.L., Osman,R. and Ross,J.B. (2001) Probing structure and dynamics of DNA with 2-aminopurine: effects of local environment on fluorescence. *Biochemistry*, **40**, 946–956.
34. Neely,R.K., Daujotyte,D., Grazulis,S., Magennis,S.W., Dryden,D.T., Klimasauskas,S. and Jones,A.C. (2005) Time-resolved fluorescence of 2-aminopurine as a probe of base flipping in M.HhaI-DNA complexes. *Nucleic Acids Res.*, **33**, 6953–6960.
35. Lakowicz,R.J. (1999) *Principles of Fluorescence Spectroscopy, 2nd edn.* Kluwer Academic/Plenum Publishers, New York.
36. Powell,L.M., Connolly,B.A. and Dryden,D.T.F. (1998) The DNA binding characteristics of the trimeric EcoKI methyltransferase and its partially assembled dimeric form determined by fluorescence polarisation and DNA footprinting. *J. Mol. Biol.*, **283**, 947–961.
37. Allan,B.W., Reich,N.O. and Beechem,J.M. (1999) Measurement of the absolute temporal coupling between DNA binding and base flipping. *Biochemistry*, **38**, 5308–5314.
38. Johnson,K.A. (1986) Rapid kinetic analysis of mechanochemical adenosinetriphosphatases. *Methods Enzymol.*, **134**, 677–705.
39. Kozlov,A.G. and Lohman,T.M. (1999) Adenine base unstacking dominates the observed enthalpy and heat capacity changes for the Escherichia coli SSB tetramer binding to single-stranded oligoadenylates. *Biochemistry*, **38**, 7388–7397.
40. Ghosh,M., Rumpal,N., Varshney,U. and Chary,K.V. (2002) Structural basis for poor uracil excision from hairpin DNA. An NMR study. *Eur. J. Biochem.*, **269**, 1886–1894.
41. Ghosh,M., Vinay Kumar,N., Varshney,U. and Chary,K.V. (2000) Structural basis for uracil DNA glycosylase interaction with uracil: NMR study. *Nucleic Acids Res.*, **28**, 1906–1912.